INTERNATIONAL JOURNAL OF
ENERGY AND ENVIRONMENT

Volume 5, Issue 3, 2014 pp.375-386
Journal homepage: www.IJEE.IEEFoundation.org

Improvement the performance of a proton exchange membrane fuel cell by changing the channel geometry

I. Khazaee

Faculty of Mechanical and Energy Engineering, Shahis Beheshti University, A.C., Tehran, Iran.

Abstract

In this study the effect of placing different blocks on the performance of a proton exchange membrane (PEM) fuel cell are investigated numerically for different Aspect Ratios. A complete two-dimensional and single phase model is used to that the proposed model is a full cell model, which includes all the parts of the PEM fuel cell, flow channels, gas diffusion electrodes, catalyst layers and the membrane. Coupled transport and electrochemical kinetics equations are solved in a single domain; therefore no interfacial boundary condition is required at the internal boundaries between cell components. The results show that the predicted polarization curves by using this model are in good agreement with the experimental results. Also the results show that the transverse installation of a rectangular and triangle block in the fuel flow channel can effectively enhance the local cell performance of a PEMFC. The results show that by increasing the aspect ratio of the blocks, the performance of the cell enhances due to enhance the electrochemical reaction at the catalyst layer of the cell.

Keywords: PEM fuel cell; Rectangular block; Triangle block; Numerical modeling; Cell performance.

1. Introduction

A fuel cell is an electro-chemical energy device that converts the chemical energy of fuel directly into electricity and heat, with water as a by-product of the reaction. Based on the types of electrolytes used, they are categorized into polymer electrolyte membrane fuel cells (PEMFCs), solid oxide fuel cells (SOFCs), phosphoric acid fuel cells (PAFCs), molten carbonate fuel cells (MCFCs), and direct methanol fuel cells (DMFCs). The polymer exchange membrane fuel cell (PEMFC) is considered to be the most promising candidate for electric vehicles by virtue of its high power density, zero pollution, low operating temperature, quick start-up capability and long lifetime. PEMFC can also be used in distributed power systems, submarines, and aerospace applications [1].

The single-cell PEMFC consists of a carbon plate, a gas diffusion layer (GDL), a catalyst layer, for each of the anode and the cathode sides, as well as a PEM membrane at the center.

Flow channel geometry is of critical importance for the performance of fuel cells containing proton exchange membranes (PEM) but is of less concern for solid oxide fuel cells (SOFC). The reactants, as well as the products, are transported to and from the cell through flow channels. Flow field configurations, including parallel, serpentine, interdigitated, and other combined versions, have been developed.

The performance of the fuel cell system is characterized by current-voltage curve *(i.e. polarization curve)*. The difference between the open circuit potential of the electrochemical reaction and cell voltage

occurs from the losses associated with the operation. The corresponding voltage drop is generally classified in three parts:
i. activation over-potential caused by the electrochemical reactions,
ii. ohmic drop across the polymer electrolyte
iii. mass transfer limitations of reactants

These associated losses dominate over different current density ranges. For low current densities; the activation over-potential is dominant. For high current densities, which are of particular interest for vehicle applications because of higher power density; the mass transfer limitations dominates the losses. For moderate current densities, the ohmic drop across the polymer membrane dominates. Moreover, for high current densities, water starts to exist in liquid form leading to a two-phase transport of reactants to reaction site, which is an additional transport phenomenon of PEM Fuel Cell operation.

West and Fuller [2] proposed a two-dimensional numerical analysis of the rib spacing in PEM electrode assemblies on current and water distribution within the cell. The results indicated that increasing the rib width strongly affected the membrane water content before the catalyst utilization is reduced. Therefore, the two-dimensional effect has a significant influence on water management.

Chiang and Chu [3] investigated the effects of transport components on the transport phenomena and performance of PEM fuel cells by using a three-dimensional model. The impacts of channel aspect ratio (AR) and GDL thickness were examined. It was found that a flat channel with a small AR or a thin GDL generates more current at low cell voltage due to the merits of better reactant gas transport and liquid water delivery.

Wang et al. [4] developed a two-dimensional numerical model to study the two-phase flow transport in the air cathode of a PEMFC. In this paper, the model encompassed both single- and two-phase regimes corresponding to low and high current densities and was capable of predicting the transition between the two regimes.

Jenn-Kun Kuo et al. [5] performed numerical simulations to evaluate the convective heat transfer performance and velocity flow characteristics of the gas flow channel design to enhance the performance of proton exchange membrane fuel cells (PEMFCs). Their study has simulated low Reynolds number laminar flow in the gas flow channel of a PEMFC. The heat transfer performance and enhanced gas flow velocity characteristics of four different channel geometries have been considered, namely a conventional straight gas flow channel and a gas flow channel with the three novel periodic patterns geometries.

The results indicated that, compared to the conventional gas flow channel, the novel gas flow channels proposed in this study provide a significantly improved convective heat transfer performance and a higher gas flow velocity and, hence, an improved catalysis reaction performance in the catalyst layer.

Based on available literature, the present study numerically investigated the effect of using rectangular and triangle baffle blocks and rectangular and triangle blocks in flow fields on cell performance and voltage losses of a PEM fuel cell. The objective of the current work is to show the effect of increasing the aspect ratio of the obstacles in the channels that it may be of interest to engineers attempting to develop the optimization of a PEMFC and to researchers interested in the flow modification aspects of the PEMFC performance enhancement.

2. Numerical model

The cathode electrochemical reactions produce a large amount of liquid water at high electric current. If the liquid water is not properly removed and accumulates in the pores of the porous layers, it restricts the oxygen transport to the gas diffusion layer and the catalyst layer, thereby reducing the electrochemical reaction rate.

The numerical model for the fuel cell used here includes the anode flow channels, anode gas diffusion layer, anode catalyst layer, proton exchange membrane, cathode catalyst layer, cathode gas diffusion layer, and cathode flow channels. Miniature fuel cells with dimensions of 4.731mm×100mm are considered in this investigation. The gas diffusion layer is 0.33mm thick, the catalyst layer is 0.01mm thick, and the proton exchange membrane is 0.051mm thick. The geometrical relations in this study are for two blocks in four aspect ratios as AR=0.2, 0.4, 0.6 and 0.8.

The physical problem considered in this paper is the two dimensional cell model of the PEMFC system as shown in Figure 1 that the dimensionless parameter in this paper named aspect ratio, $AR = \frac{L}{H}$, is defined to characterize the blockage effect of the blocks.

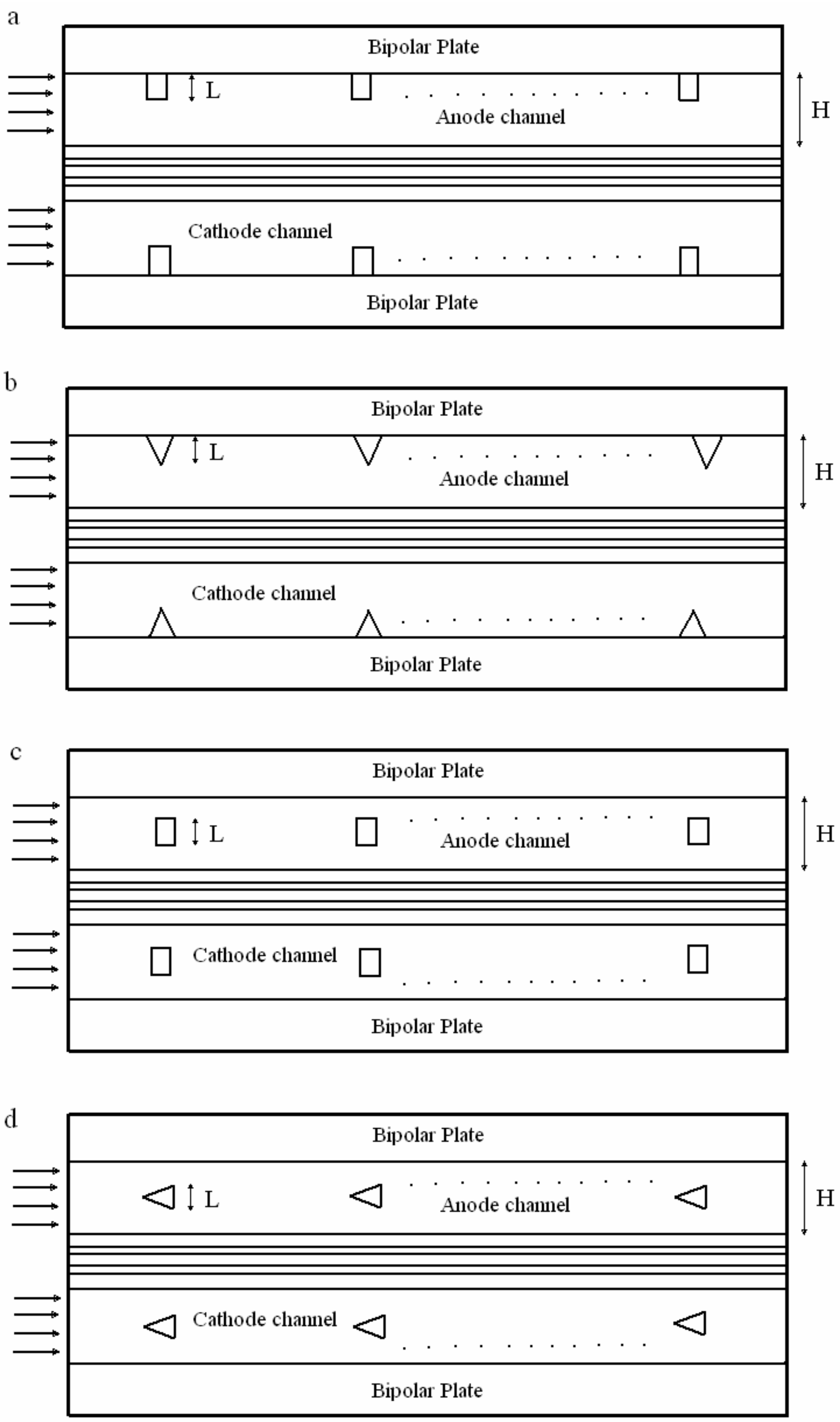

Figure 1. Computational domain of PEMFC with (a) rectangular baffle block, (b) triangle baffle block, (c) rectangular block and (d) triangle block

The proposed model that described in previous work [6] does not require any internal boundary conditions between the components of PEM Fuel Cell system. The different physical properties and transport parameters are incorporated into a single set of governing equations using a single domain formulation. The model aims to study the electrochemical kinetics, current distribution, reactant flow fields and multi-component transport of oxidizer and fuel streams in a multi-dimensional domain. The assumptions made in developing the model are as follows:

- Ideal gas mixtures
- Incompressible and Laminar flow because low flow velocities and low fuel utilization
- Isotropic and homogeneous porous electrodes, catalyst layers and membrane
- Isothermal operation
- Negligible ohmic resistance at porous electrodes and current collectors

The model assumes that the system is steady; the inlet reactants are ideal gases; the flow is laminar; and the porous layers such as the diffusion layer, catalyst layer and PEM are isotropic. The model includes continuity, momentum and species equations for gaseous species, liquid water transport equations in the channels, gas diffusion layers, and catalyst layers, water transport equation in the membrane, electron and proton transport equations. The Bulter–Volumer equation was used to describe electrochemical reactions in the catalyst layers.

The conservation equations of mass, momentum, species and charge are as follows:

$$\frac{\partial(\rho\varepsilon)}{\partial t}+\nabla.(\varepsilon\rho\vec{u})=0 \tag{1}$$

$$\frac{\partial(\rho\varepsilon\vec{u})}{\partial t}+\nabla.(\varepsilon\rho\vec{u}\vec{u})=-\varepsilon\nabla p+\nabla.(\varepsilon\mu\nabla\vec{u})+S_u \tag{2}$$

$$\frac{\partial(\varepsilon X_k)}{\partial t}+\nabla.(\varepsilon\vec{u}X_k)=\nabla.(D_k^{eff}\nabla X_k)+S_k \tag{3}$$

$$\nabla.(\sigma_g^{eff}\nabla\phi_e)+S_\phi=0 \tag{4}$$

where $\vec{u}, X_k and \phi_e$ denotes intrinsic velocity vector, molar fraction of k^{th} species and electrolyte phase potential, respectively. The corresponding source terms treating the electrochemical reactions and porous media are presented in Table 1.

Table 1. Source terms

	S_v (Momentum)	S_k (Species)	$S_Ø$ (Phase potential)
Gas channels	0		
Backing layers	$-\frac{\mu}{k}\varepsilon^2\vec{u}$		
Catalyst layers	$-\frac{\mu}{k}\varepsilon^2\vec{u}$	$-\frac{j_a}{2F}\frac{\rho}{\varepsilon_m\varepsilon_{mc}}$: anode H_2 $\frac{j_c}{2F}\frac{\rho}{\varepsilon_m\varepsilon_{mc}}$: cathode O_2 $-\frac{j_c}{F}\left(\frac{1}{2}+n_d\right)\frac{\rho}{\varepsilon_m\varepsilon_{mc}}$: cathode H_2O $-\frac{n_d}{F}j_a\frac{\rho}{\varepsilon_m\varepsilon_{mc}}$: anode H_2O	j
Membrane	$-\frac{\mu}{k}\varepsilon^2\vec{u}$		

It is of benefit to further explain the corresponding diffusivities of the governing equations. The diffusivities for species concentration equations and ionic conductivity for membrane phase potential equation are modified using Bruggman correlation to account for porous electrodes, which can be expressed as:

$$D_k^{eff} = \varepsilon_m^{1.5} D_k \tag{5}$$

$$\sigma_e^{eff} = \varepsilon_m^{1.5} \sigma_e \tag{6}$$

It is worth further explaining the mole fraction of oxygen appearing in Eq. 3 because oxygen is a gaseous species in the cathode flow channel and gas-diffusion electrode but becomes a species dissolved in the electrolyte in the catalyst layer and membrane regions. Our definition is given by

$$X_k = \begin{cases} C_k^g / C_{tot} & in\ gas \\ C_k^e / C_{tot} & in\ electrode \end{cases} \tag{7}$$

where C_k is the molar concentration of species k and superscripts g and e denote the gas and the electrolyte phases, respectively. Thus, X_k is a true mole fraction in the gas phase but is a pseudo mole fraction when species k is in the dissolved form. In addition, there is a discontinuity in the value of X_k at the interface between the gas-diffusion electrode and the catalyst layer due to the following thermodynamic relation

$$C_k^{e,sat} = \frac{RT}{H} C_k^g \tag{8}$$

where H is the Henry's law constant equal to $2 \times 10^5\ atm\ cm^3 / mol$ for oxygen in the membrane.

Either generation or consumption of chemical species k and the creation of electric current occurs only in the active catalyst layers where electrochemical reactions take place. The S_k and S_ϕ terms are therefore related to the transfer current between the solid matrix and the membrane phase inside each of the catalyst layers. These transfer currents at anode and cathode can be expressed as follows

$$j_a = a j_{0,a}^{ref} \left(\frac{X_{H_2}}{X_{H_2,ref}} \right)^{1/2} \left(\frac{\alpha_a + \alpha_c}{RT} .F.\eta \right) \tag{9}$$

$$j_c = -a j_{0,c}^{ref} \left(\frac{X_{O_2}}{X_{|O_2,ref}} \right)^{1/2} \left(-\frac{\alpha_c .F}{RT} .\eta \right) \tag{10}$$

The above kinetics expressions are derived from the general Bulter- Volmer equation based on the facts that the anode exhibits fast electrokinetics and hence a low surface overpotential to justify a linear kinetic rate equation, and that the cathode has relatively slow kinetics to be adequately described by the Tafel equation. In Eq. 9 and 10, the surface overpotential, $\eta(x, y)$, is defined as

$$\eta(x, y) = \phi_s - \phi_e - V_{oc} \tag{11}$$

where ϕ_S and ϕ_ε stand for the potentials of the electronically conductive solid matrix and electrolyte, respectively, at the electrode electrolyte interface. V_{OC} is the reference open-circuit potential of an electrode. It is equal to zero on the anode but is a function of temperature on the cathode namely

$$V_{oc} = 1.17 - 2.756 \times 10^{-4} (T - 373.15) + 4.308 \times 10^{-5} \ln \left(\frac{a_{H_2} (a_{O_2})^{1/2}}{a_{H_2O}} \right) \tag{12}$$

where T is in Kelvin and V_{oc} is in volts. Notice that V_{oc} is not the true open-circuit potential of an electrode, which would then depend upon reactant concentrations according to the Nernst equation.
This equilibrium potential is calculated from thermodynamic data of reaction enthalpy and entropy changes while the product water is in gaseous phase. The definition of a_{H_2}, a_{O_2} and a_{H_2O} are:

$$a_{H_2O} = \frac{p_{H_2}}{p^0}, \qquad a_{O_2} = \frac{p_{o_2}}{p^0}, \qquad a_{H_2O} = \frac{p_{H_2O}}{p^0_{H_2O}}. \tag{13}$$

The dependence of the cathodic exchange current density on temperature can be fitted as

$$\frac{i_0(T)}{i_0(353K)} = \exp(0.014189(T-353)) \tag{14}$$

The species diffusivity, D_k, varies in different subregions of the PEMFC depending on the specific physical phase of component k. In flow channels and porous electrodes, species k exists in the gaseous phase, and thus the diffusion coefficient takes the value in gas, whereas species k is dissolved in the membrane phase within the catalyst layers and the membrane, and thus takes the value corresponding to dissolved species, which is usually a few orders of magnitude lower than that in gas. In addition, the diffusion coefficient is a function of temperature and pressure.

$$D(T) = D_0\left(\frac{T}{T_0}\right)^{3/2}\left(\frac{p_0}{p}\right) \tag{15}$$

The proton conductivity in the membrane phase has been correlated as

$$\sigma_e(T) = 100\exp\left[1268\left(\frac{1}{303} - \frac{1}{T}\right)\right](0.005139\xi - 0.00326) \tag{16}$$

where the water content in the membrane, ξ, depends on the water activity, a, according to the following fit of the experimental data

$$\xi = \begin{cases} 0.043 + 17.18a - 39.85a^2 + 36a^3 & 0 \prec a \le 1 \\ 14 + 1.4(a-1) & 1 \le a \le 3 \end{cases} \tag{17}$$

The water activity is in turn calculated by

$$a = \frac{X_{H_2O}\,p}{p_{sat}} \tag{18}$$

where the saturation pressure of water vapor can be computed from the following empirical equation

$$\ln(p^{sat}) = 70.43464 - \frac{7362.698}{T} + 0.006952T - 9\ln(T) \tag{19}$$

In a fuel cell system, the inlet flow rates are generally expressed as stoichiometric ratios of inlet streams based on a reference current density. The stoichiometric ratios inlet streams are given by the following equations.

$$S^{anode} = C_{H_2} v^{anode} \frac{2F}{I_{ref} A} \tag{20}$$

$$S^{cathode} = C_{O_2} v^{cathode} \frac{4F}{I_{ref} A} \tag{21}$$

Water transport through the polymer electrolyte membrane has been investigated by several researchers in different aspects. Most interesting studies in this area includes the determination of water diffusion coefficient [7] and water drag coefficient [8] by Zawodzinski et al. and investigating the diffusion of water in Nafion membranes by Motupally et al.[9].

The electro-osmotic drag coefficient is defined as the number of water molecules transported by each hydrogen proton H^+. The electro-osmotic drag coefficient can be expressed with the following equation:

$$n_d = \frac{2.5\xi}{22} \tag{22}$$

The diffusion coefficient of water in Polymer Membrane is also highly dependent on the water content of the membrane. The relation is given as:

$$D_w^m = \begin{Bmatrix} 3.1\times10^{-7}\xi(\exp(0.28\xi)-1)\exp(-2346/T) & 0 \prec \xi \prec 3 \\ 4.17\times10^{-8}\xi(1+161\exp(-\xi))\exp(-2346/T) & otherwise \end{Bmatrix} \tag{23}$$

Once the electrolyte phase potential is determined in the membrane, the local current density along the axial direction can be calculated as follows

$$I(y) = -\sigma_e^{eff} \frac{\partial\phi_e}{\partial x}\bigg|_{x=I.F.} \tag{24}$$

where I.F. means the interface between the membrane and cathode catalyst layer. The average current density is then determined by

$$I_{avg} = \frac{1}{L}\int_0^L I(y)dy \tag{25}$$

where *L* is the cell length.

The boundary conditions prescribed at the inlets of the gas channels are:

$$\begin{array}{ll} u_{in}^{anode} = u_a^0 & u_{in}^{cathode} = u_c^0 \\ C_{H_2}^{anode,in} = C_{H_2}^0 & C_{O_2}^{cathode,in} = C_{O_2}^0 \\ C_{H_2O}^{anode,in} = C_{H_2O}^{0,a} & C_{H_2O}^{cathode,in} = C_{H_2O}^{0,c} \end{array}$$

A mesh of 241×74×25 was found to provide required spatial resolution for four-channel geometry. The solution is considered to be converged when the difference between successive iterations is less than 10^{-7} for all variables.

The Electrochemical and Transport Parameters used in these simulations are summarized in Table 2, and the operational parameters are presented in Table 3.

Table 2. Electrochemical and transport properties

Description	Unit	Value
Anode reference exchange current density	A/m^3	1.5e9
Cathode reference exchange current density	A/m^3	4000000
Anode transfer coefficient		2
Cathode transfer coefficient		2
Faraday constant	C/mol	96487
H_2 Diffusivity	m^2/s	3e-5
O_2 Diffusivity	m^2/s	3e-5
H_2O Diffusivity at anode	m^2/s	3e-5
H_2O Diffusivity at cathode	m^2/s	3e-5
Anode backing layer porosity		0.5
Cathode backing layer porosity		0.5
Permeability of anode backing layer	m^2	e-12
Permeability of cathode backing layer	m^2	e-12
Equivalent weight of membrane	kg/mol	1.1

Table 3. Operational parameters

Description	Unit	Value
reference average current density	A/cm^2	1.0
Anode inlet velocity	m/s	3
Cathode inlet velocity	m/s	2
Anode inlet pressure	Atm	1
Cathode inlet pressure	Atm	1
Cell temperature	C°	70
Anode inlet molar concentration		
Hydrogen	mol/m^3	35.667
Oxygen	mol/m^3	0
Water vapor	mol/m^3	16.121
Cathode inlet molar concentration		
Hydrogen	mol/m^3	0
Oxygen	mol/m^3	0 7.51
Water vapor	mol/m^3	16.121

4. Results and discussion

In order to show that the program in this study can handle the cell performance of a PEMFC, we apply the present method to solve the whole of a PEMFC as described in Miansari and others ’ paper [10]. The physical parameters and properties of the fuel cell are listed in Table 2. The mesh employed for the comparison with the reference was 241×74×25. The steady-state solution is obtained by the numerical procedure as mentioned in the previous section. As shown in Figure 2, the result of the present predictions of the polarization curve agreeing fairly closely with Miansari and others’ predictions [10] gives one confidence in the use of the present program.

Figure 3 (triangle block and triangle baffle block) and Figure 4 (rectangular block and rectangular baffle block) illustrate the polarization curves of the fuel cell performance for different channel geometries with nine blocks (n=9) to investigate the influence of the internal flow modification on the overall fuel cell performance. An overall inspection of Figures 3 and 4 indicates that at the conditions of the higher operating voltage (lower over- potential), the influence of the internal flow modification on the overall fuel cell performance is negligibly small. At lower operating voltage conditions, on the other hand, the effect of the internal flow modification on the polarization curves becomes important. Also Figures 3(a),(b) and 4(a),(b) show that the influence of baffle block on the overall fuel cell performance is small. In addition, for the installation of triangle and rectangular blocks, the overall cell performance decreases when the aspect ratio *AR* decreases. This is due to the fact that a reflection of the more efficient fuel transport and the chemical reaction around the triangle and rectangular blocks reduces the local current density more obviously in the downstream region behind the triangle and rectangular blocks.

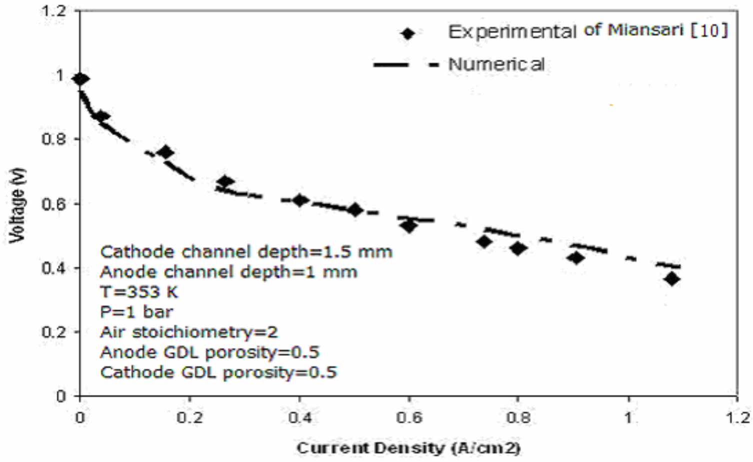

Figure 2. Comparison between results of this paper and results of Miansari et al [10]

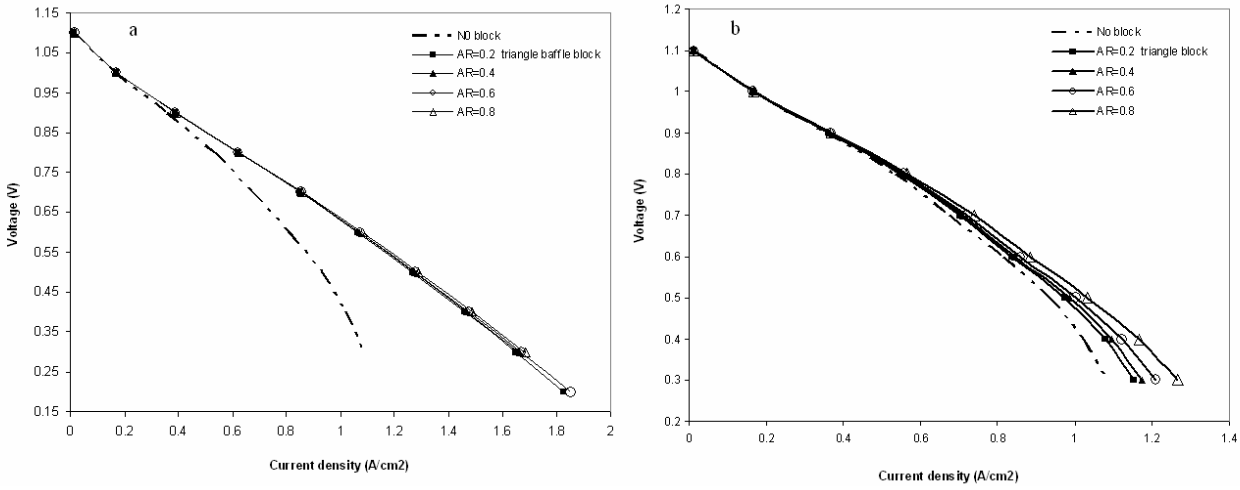

Figure 3. Variation of cell performance at different AR for (a) triangle baffle block and (b) triangle block

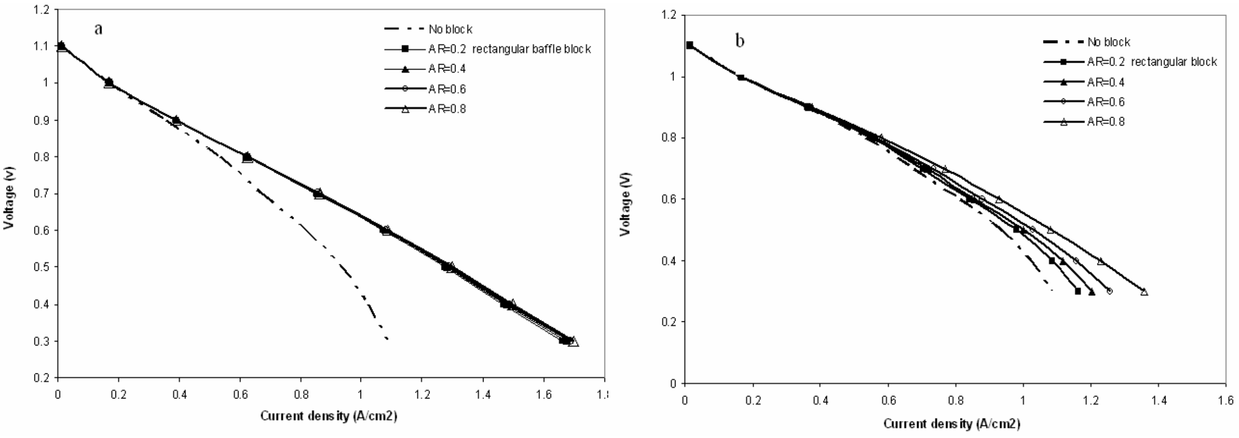

Figure 4. Variation of cell performance at different AR for (a) rectangular baffle block and (b) rectangular block

Figure 5 shows the polarization curves of the fuel cell performance for seven different channel geometries with n=0, n=9, n=13 and n=24 for AR=0.8 to investigate the influence of the internal flow modification on the overall fuel cell performance. It is clear that by increasing the number of the blocks in the channels and installation of rectangular block, the overall cell performance increases. This is due to the fact that a reflection of the more efficient fuel transport and the chemical reaction around the rectangular block reduces the local current density more obviously in the downstream region behind the rectangular block. Also it is clear that the performance of the cell is at higher value by rectangular block with n=9 than triangle block with n=13, therefore there is a best condition for lower capital cost of the fuel cell.

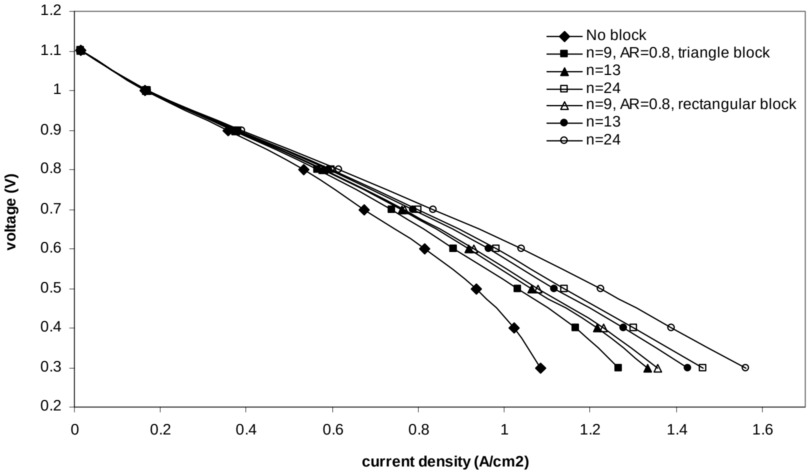

Figure 5. Variation of cell performance for n=0, n=9, n=13 and n=24 and AR=0.8 for triangle and rectangular block

The effect of kind of blocks in the channels presented in Figure 6 for n=9 and AR=0.2, 0.4, 0.6 and 0.8. It is clear that by increasing the aspect ratio of the blocks in the channel, the overall performance of the cell increases but the difference between the performance of the cell at a constant AR for rectangular block than triangle block is very high that this is due to more decreases of local current density in the downstream region behind the rectangular block. Also it is clear that at the conditions of the higher operating voltage (lower over- potential), the influence of the internal flow modification on the overall fuel cell performance is negligibly small and at lower operating voltage conditions the effect of the internal flow modification on the polarization curves becomes important.

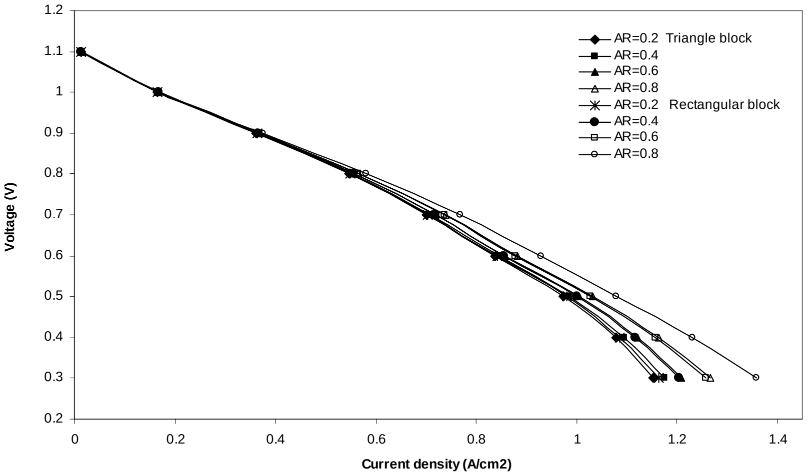

Figure 6. Comparison of cell performance between triangle block and rectangular block for different AR

In Figures 7 and 8, the local current density along the catalyst surface decreases when the axial direction *x* increases except for the peak regions but for triangle and rectangular baffle blocks it increases in the downstream region behind the baffle blocks. Also it is clear that the local current density is at higher value for baffle blocks that it is due to the more blockage of the fuel gas around the baffle blocks and forcing the more fuel gas into the gas diffusion layer to enhance the chemical reaction at the catalyst layer. The local current density around the baffle blocks and blocks increases with increasing the aspect ratio (AR), and the difference of the peak regions between the baffle blocks and the blocks is very high and also the difference between the triangle block and rectangular block is very high. These peak regions of the distribution of the local current density are caused by the transverse installation of a baffle blocks and blocks. This phenomena means that better cell performance is achieved around the baffle blocks or blocks. This is due to the fact that the fuel gas is blocked by the blocks installed in the flow channel, and more fuel gas is forced into and passes through the gas diffusion layer, which enhances the chemical reaction at the catalyst surface.

In the downstream region behind the baffle blocks and blocks, the local current density decreases as the aspect ratio (AR) decreases. The reduction of the local current density is because of increasing the fuel velocity and decreasing the chemical reaction and less flow into the GDL in the downstream region behind the baffle blocks and blocks. But the difference between current density behind the blocks is very high for triangle and rectangular blocks than the triangle and rectangular baffle blocks.

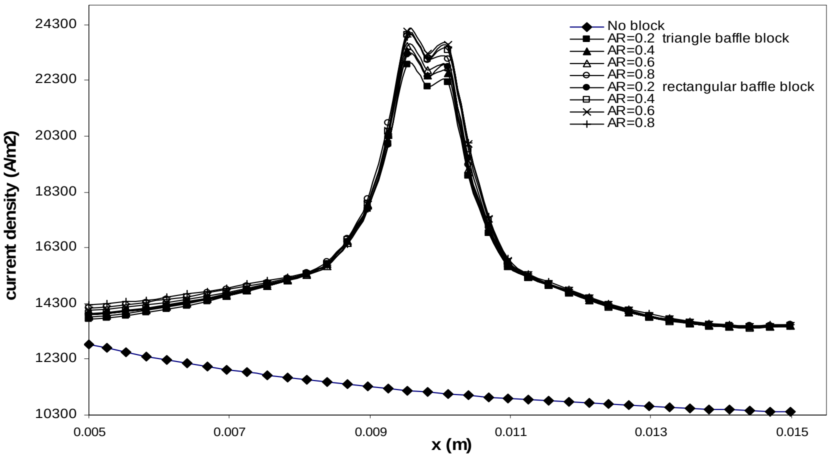

Figure 7. The local current density distributions along the catalyst surface for different AR and triangle and rectangular baffle blocks

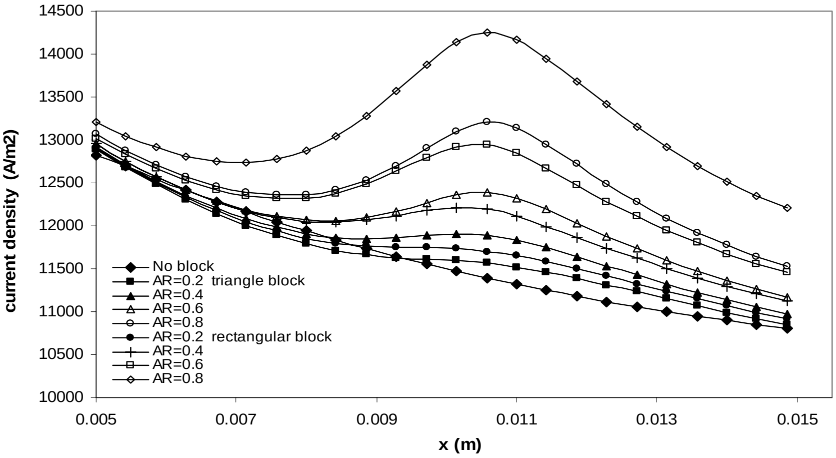

Figure 8. The local current density distributions along the catalyst surface for different AR and triangle and rectangular blocks

5. Conclusion

A complete two-dimensional and single phase model for proton exchange membrane (PEM) fuel cells has been used to investigate the effect of placing triangle and rectangular baffle blocks and triangle and rectangular blocks in the flow channels on the performance for different aspect ratios. The complete two-dimensional model for PEM fuel cells based on the two-fluid method was numerically solved with constant-temperature boundary condition at surfaces of anode and cathode current collectors. The results of this paper are in good agreement with experimental results of miansari et al[10]. The results show that by installing the baffle blocks or blocks into the channels and by increasing the aspect ratio of the blocks the overall cell performance increases. Also the results show that the difference between the performance of the cell at a constant AR for rectangular block than triangle block is very high and by increasing the number of the blocks in the channels and installation of rectangular block, the overall cell performance increases. The local current density is at higher value for baffle blocks than blocks by increasing the AR that it is due to the more blockage of the fuel gas around the baffle blocks and forcing the more fuel gas into the gas diffusion layer. however, the installation of rectangular baffle blocks and rectangular blocks have better overall cell performance than the installation of triangle baffle blocks and triangle blocks and enhances the overall cell performance of a PEMFC system.

Nomenclature

A	Superficial electrode area, m^2
C	Molar concentration, mol/m^3
D	Species diffusivity, m^2/s
I	Current density, A/cm^2
i_0	Reference current density, A/cm^2
U	Inlet velocity, m/s
j	Transfer current density, A/m^3
$\vec{u}$	Velocity vector, m/s
P	pressure, Pa
p^0	Reference pressure, Pa
S	Stoichiometric Ratio
T	Temperature, K

Greek letters

η	Overpotential, V
ρ	Density, kg/m^3
ε	Porosity
σ	Ionic conductivity, S/m
ϕ	Phase potential, V
ν	Volumetric flow rate, m^3/s
ξ	Water content of the membrane
μ	Viscosity, kg m/s
α	Transfer coefficient for the reaction

Acknowledgment

This work was partially supported by Renewable Energy Organization of Iran.

References

[1] J. Larminie, and A. Dicks, Fuel cell system explained., John Wiley and Sons.,2nd edition, 2003.

[2] A.C. West, and T.F. Fuller, "The Influence of Rib Spacing in Proton-Exchange Membrane Electrode Assemblies", Journal of Applied Electrochemistry, 26(1996), pp. 557–565.

[3] M.S. Chiang, and H.S. Chu, "Transient behavior of CO poisoning of the anode catalyst layer of a PEM fuel cell", Journal of Power Sources, 160 (2006), pp.340–352.

[4] Z.H. Wang, C.Y. Wang, and K.S. Chen, "Two-phase flow and transport in the air cathode of proton exchange membrane fuel cells", Journal of Power Sources, 94 (2001), pp.40–50.

[5] J.K. Kuo, T.S. Yen, and C.K. Chen, "Improvement of performance of gas flow channel in PEM fuel cells", Energy Conversion and Management, 49 (2008), pp.2776–2787.

[6] I. Khazaee, and M. Ghazikhani, "Performance improvement of proton exchange membrane fuel cell by using annular shaped geometry", Journal of Power Sources, 196(2011), pp.2661-2668.

[7] T.A. Zawodzinski, M. Neeman, L.O. Sillerud, and S. Gottesfeld, "Determination of water diffusion coefficients in perfluorosulfonate ionomeric membranes", The Journal of Physical Chemistry, 95 (1991), pp.6040-6044.

[8] T.A. Zawodzinski, J. Davey, J. Valerio, and S. Gottesfeld, "The water content dependence of electro-osmotic drag in proton-conducting polymer electrolytes", Electrochimica Acta, 40 (1995), pp.297-302.

[9] S. Motupally, A.J. Becker, and J.W. Weidner, "Diffusion of Water through Nafion® 115 Membranes", Journal of the Electrochemical Society, 147 (2000), pp.3171-3177.

[10] ME. Miansari, K. Sedighi, M. Amidpour, E. Alizadeh, and MO. Miansari, "Experimental and thermodynamic approach on proton exchange membrane fuel cell performance", Journal of Power Sources, 190 (2009), pp.356-361.

Iman Khazaee was born in mashhad, iran, in 1983. He received his B.S. degree in mechanical engineering from Ferdowsi university of mashhad in 2006 and his master's degree at mechanical engineering department, Amirkabir University of Technology in 2008 and a PhD degree from Ferdowsi University of Mashhad in 2011. Currently, he is working on PEM fuel cells and their optimization.
E-mail address: Imankhazaee@yahoo.com